ISBN: 978-3-95450-208-0 doi:10.18429/JACoW-IPAC2019-TUPGW080

ALTERNATIVE LATTICE DESIGN FOR DIAMOND-II

M. Korostelev[1,2], B. Singh[2]
[1]Oxford University, Physics Department, Oxford, UK
[2]Diamond Light Source Ltd (DLS), Didcot, UK

Abstract

Plans for upgrade of the Diamond Light Source aim to reduce beam emittance by a factor of 20 or better. This is motivated by demand for photon flux with significantly high brightness and transverse coherence. The baseline lattice design for the Diamond-II upgrade has been recently proposed, however alternative design are under investigation to reduce the emittance even further. This paper presents a new lattice design based on implementation of bending magnets with transverse field gradient only.

INTRODUCTION

The brightness and coherent fraction of the photon beams for Diamond-II Synchrotron Light Source upgrade will be significantly increased, compared to the existing Diamond light source due to the reduction in electron emittance. The concept of a so-called Modified Hybrid-Multi-Bend-Achromat (M-HMBA) cell design was proposed for the Diamond-II lattice. This cell is based on the H7BA lattice designed for the ESRF-EBS upgrade [1] from which the central dipole has been removed. The baseline M-H6BA lattice design for the Diamond-II has been reported in the CDR [2] and features bending dipoles with longitudinal field gradient and introduces an additional 24 new mid-straight section that can be used for short in vacuum insertion devices. It has been recently proposed to operate Diamond-II at 3.5 GeV instead of 3 GeV. The M-H6BA lattice delivers a natural emittance of 160 pm at 3.5 GeV, 17 times lower than that of the existing machine (2700 pm), comparing the bare lattices.

In order to decrease further the emittance, alternative lattice designs for Diamond-II are under investigation. We developed a new ultra-low emittance lattice (named 'M-6BA') based on Modified Six-Bend-Achromat (M-6BA) cell with dispersion free mid-straight section (inside the cell), implementing bending magnets with transverse field gradient only. The M-6BA lattice provides a natural emittance of 115 pm at 3.5 GeV, 23 times lower than the existing machine (compared to bare lattices). The M-6BA lattice design meets the engineering requirements for arrangement of the storage ring in the existing tunnel, and also meets other engineering constraints specified for the Diamond-II upgrade.

LATTICE DESIGN

The M-6BA lattice has been designed with 24 M-6BA cells in a circumference of 561 m and maintains the 6-fold symmetry of Diamond with a long straight section (LS) every four cells. One LS section is equipped with a septum and kicker magnets for injection, one LS with RF cavities, the other four LS contains IDs. Figure 1 shows the optics functions in one super-period. Each M-6BA cell is composed from two identical Triplet Bend Achromats (TBA) connected by a dispersion-free mid-straight section (MS) 2.9 m of long (quad-to-quad) with a doublet of quadrupoles on both ends. In order to provide a good flexibility in tuning for optics and phase advance over the straights, triplets are used in the standard straight section (SS) and LS section. Figure 2 shows the TBA structure which is mirror symmetric with respect to the central dipole DQ. Each TBA includes three chromatic sextupole families (SF, SD and SD1) to control 1st and 2nd order chromaticities. One family of octupoles is used to control mainly the dQ_x/dA_x amplitude dependent tune shift. Harmonic sextupoles are not used in the lattice. Table 1 summarizes the main lattice parameters.

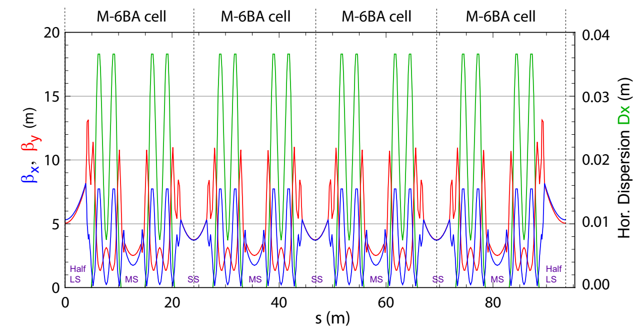

Figure 1: Optics functions in the super-period.

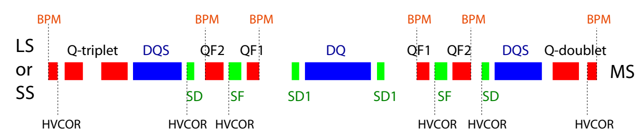

Figure 2: Half of the M-6BA cell.

Optimization of non-linear optics is always the challenge for ultra-low emittance lattices due to strong non-linearities introduced by the sextupoles. $-I$ transformers between sextupole pairs in each M-6BA cell are implemented to provide cancellation of the 1st order geometric terms of sextupoles which drive 3rd order resonances. Further attempts were made to minimize the 2nd order geometric terms over two super-periods. The on-momentum dynamic aperture (top plot) and off-momentum dynamic aperture for momentum deviation of ±2% (middle plot) and ±3% (bottom plot) have been calculated from particle tracking using the Elegant code [3], as shown in Fig. 3.

ISBN: 978-3-95450-208-0 doi:10.18429/JACoW-IPAC2019-TUPGW080

Table 1: Main Lattice Parameters without IDs

Parameter	
Energy	3.5 GeV
Emittance	115 pm
Circumference	561 m
Momentum compaction	0.71×10^{-4}
Energy loss per turn	0.8 MeV
Energy spread	0.083 %
Horizontal damping partition	1.44
Damping times $\tau_x \setminus \tau_y \setminus \tau_p$	11.8\ 17.1\10.9 ms
Horizontal tune	75.67
Vertical tune	27.91
Horizontal natural chromaticity	-211
Vertical natural chromaticity	-106
RF frequency	500 MHz
Harmonic number	934
Bunch length at 1.75 MV	2.5 mm
Length of MS\SS\LS	2.9\4.9\7.8 m

LATTICE IMPERFECTIONS AND CORRECTION

Beam position monitors (BPMs) and combined horizontal and vertical dipole correctors (HVCORs) are distributed along the cell, as shown in Fig. 2. There are 288 HVCOR correctors and 288 BPMs in total; 192 correctors are embedded in the sextupoles (8 per cell) as additional windings.

We use reduced set of alignment and field errors summarized below:
Δx = 15μrad, Δy = 15μrad, Roll angle (tilt) = 100 μrad and FSE (fractional strength error) = 1×10^{-3}, to simulate the effect of residual (post-correction) closed orbit distortions, after the beam-based alignment and optics correction have been applied. The values above are the rms of a Gaussian distribution. In our simulations, no girders have been implemented, so the misalignment of magnets are uncorrelated.

A global closed orbit correction has been been performed with 20 different seeds of random errors generated on all the bending magnets, quadrupole and sextupole magnets with a Gaussian distribution (cut off at $\pm 2\sigma$). Skew quadrupoles have not been used in the correction procedure. Table 2 summarizes the rms and maximum values of the orbit deviation, residual vertical dispersion and beta-beating at different elements and sections of the machine after the closed orbit correction. The rms orbit deviation along the ring is 14.8 μm in horizontal and 3.1 μm in vertical plane, while the vertical dispersion is zero on average with rms 2.2 μm. In spite of the fact that there are some spikes of horizontal orbit deviation in the triplets, the maximum value of orbit deviation throughout the straight sections does not exceed 7 μm. The rms and maximum values of residual horizontal dispersion along the MS, SS, LS, injection section (INJ), and in the injection point are 4 μm (1.3 μm rms), 5 μm (2.0 μm rms), 5 μm (2.2 μm rms), 5 μm (3.7 μm rms), 5 μm (3.7 μm rms), respectively.

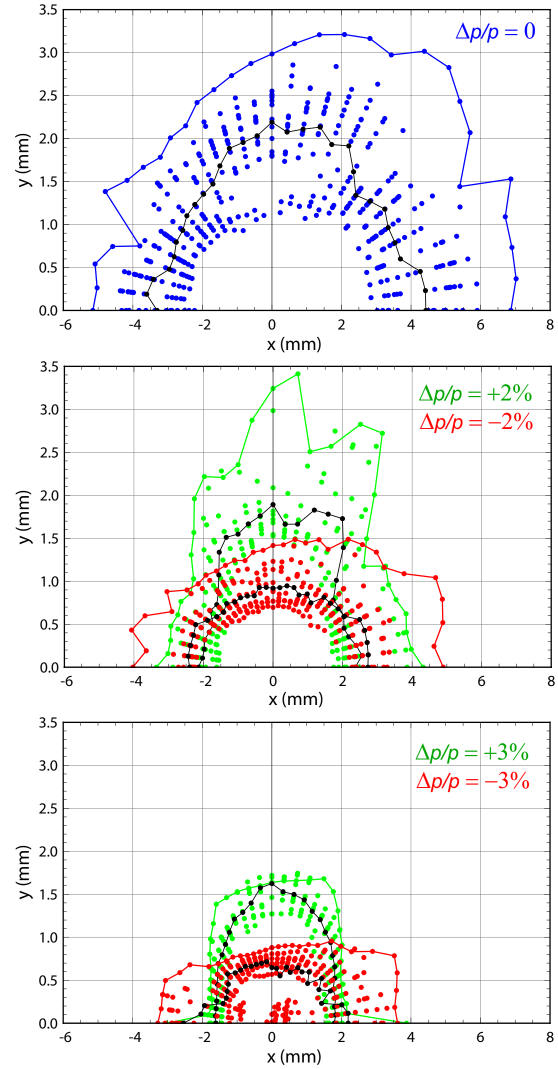

Figure 3: On-momentum DA (top), off-momentum DA at $\Delta p/p = \pm 2\%$ (middle) and $\Delta p/p = \pm 3\%$ (bottom). Solid lines in colour correspond to the DA calculated without any lattice errors. Points show the variations of the DA computed for ten seeds of the reduced errors, while solid black lines represent the DA averaged over the seeds.

The rms horizontal and vertical kicks of the correctors are 36 μrad and 20 μrad, respectively. The maximum horizontal kick over 20 seeds is less than 155 μrad, while the maximum vertical kick is less than 68 μrad.

Dynamic Aperture

The dynamic aperture (DA) demonstrates reasonable tolerance to the beta-beating, originating mainly from quadrupole field errors and sextupole-magnets misalignment. The points in Fig. 3 (top) show the variations of the footprint of the on-momentum DA computed for ten seeds. The mean on-momentum DA (solid black line) is ±4 mm in the horizontal and ±2 mm in the vertical planes. The variations for off-momentum DA at $\Delta p/p = \pm 2\%$ and $\Delta p/p = \pm 3\%$ computed for the same number of seeds and rms errors are in-

ISBN: 978-3-95450-208-0 doi:10.18429/JACoW-IPAC2019-TUPGW080

Table 2: RMS and maximum values of orbit deviation, residual vertical dispersion D_y and beta-beating after the closed orbit correction.

	X rms\max [μm]	**Y** rms\max [μm]	**β-beat** rms\max [%]	**D_y** rms\max [mm]
SEXTs	2.8\15	2.8\10	5\17	1.9\5
QF1&QF2	2.5\12	1.7\8	5\17	1.4\4
Triplets	29\150	3.7\20	5\18	2.5\8
DQS	28\100	6.2\20	5\17	2.8\6
DQ	2.2\7	4.8\10	5\17	1.6\3
BPMs	0.8\1.5	0.04\0.3	5\16	1.4\5
HVCORs	2.3\10	2.4\10	5\16	2.2\6
MS	1.4\6	0.1\0.3	5\16	1.7\4
SS	2.0\7	0.1\0.3	5\16	2.4\5
LS	2.5\7	0.1\0.3	5\16	2.8\5
INJ	3.9\12	0.2\0.4	6\14	2.9\5
INJ point	3.9\9	0.2\0.4	6\13	2.8\4
RING	14.8\150	3.1\20	5\17	2.2\8

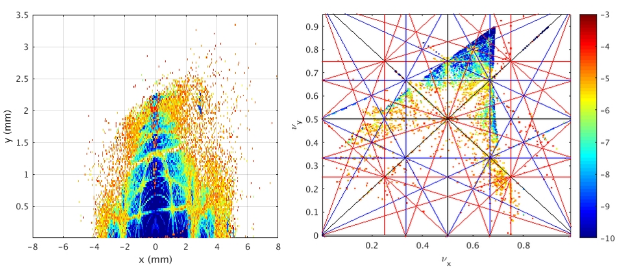

Figure 4: On-momentum diffusion map (left) and corresponding tune footprint (right) performed for one representative seed.

dicated by the points in Fig. 3 (middle and bottom plots) in which the solid black lines represent the mean value.

Figure 4 shows the on-momentum tune footprint in the tune diagram and the diffusion map of the DA as a result of tracking performed for one representative seed.

Momentum Acceptance and Touschek Lifetime

Figure 5 shows the momentum acceptance (MA) along the ring, obtained from particle tracking for the lattice with and without errors. Assuming nominal total current of 300 mA stored in 934 bunches (uniform fill pattern for 500 MHz), the Touschek lifetime calculated from the obtained MA reaches a maximum at RF voltage of 1.75 MV which is about 3.8 hours if the vertical emittance is 8 pm (the operational emittance in the existing Diamond machine). The RF voltage of 1.75 MV corresponds to 4.4% RF acceptance (red line in Figure 5). A lower vertical emittance, for example, 3.5 pm (calculated from residual vertical dispersion in our simulations) results in the Touschek lifetime of 2.5 hours at the same RF voltage.

The lattice errors after closed orbit correction reduces the MA to the limits from −3.9% to 3.3% in the injection point and ±2.2% in the arcs, as can be seen in Figure 5. This reduces the Touschek lifetime to 3 hours ± rms 0.4 and 2.1 hours ± rms 0.32 for a beam with a vertical emittance of 8 pm and 3.5 pm, respectively. The rms bunch length is 2.5 mm at the RF voltage of 1.75 MV.

There is relatively little impact on the horizontal emittance after the correction. So, a maximum emittance increase is less than 3 pm. However, at the nominal current of 300 mA and vertical emittance of 8 pm, the effects of intra-beam scattering calculated by the Bjorken and Mtingwa's formula [4] lead to the increase of both horizontal emittance and energy spread by roughly 11%, compared to their values at zero beam current, while the rms bunch length increases to 2.8 mm.

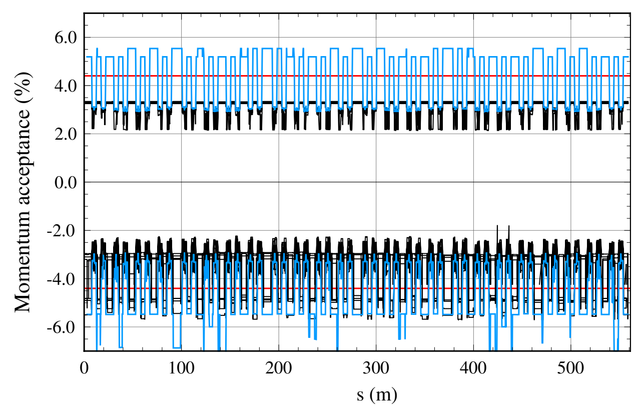

Figure 5: Momentum acceptance along the lattice with errors (black lines) and without errors (blue line). Red lines represent momentum acceptance from RF with 1.75 MV.

CONCLUSIONS

The M-6BA lattice has been developed as a low emittance alternative to the present baseline lattice design for Diamond-II. The lattice is based on 48 identical TBA structures incorporated into 24 six-BA cells, and it meets known engineering specifications. Bending magnets with transverse field gradient are the only type of dipole in the lattice. A natural beam emittance of 115 pm has been achieved, but the strong focusing of the lattice produce a big horizontal natural chromaticity. As a consequence, strong sextupole magnets for chromaticity correction are required. The dynamic aperture of the lattice is close to the threshold for off-axis injection into the Diamond-II storage ring. Tuning the lattice for symmetry in terms of phase advance between the TBA central dipole and the center of adjacent straight sections tends to improve the off-momentum DA. Further optimization of the lattice is needed to reduce the natural chromaticity and amplitude dependent tune shifts.

ISBN: 978-3-95450-208-0 doi:10.18429/JACoW-IPAC2019-TUPGW080

REFERENCES

[1] P. Raimondi, "The ESRF Low-emittance Upgrade", in *Proc. 7th Int. Particle Accelerator Conf. (IPAC'16)*, Busan, Korea, May 2016, pp. 2023–2027. doi:10.18429/JACoW-IPAC2016-WEXA01

[2] L.C. Chapon, A.J. Dent, A. Harrison, M. Launchbury, D.I. Stuart, R.P. Walker, "Diamond-II Conceptual Design Report", Diamond Light Source, 2019, to be published.

[3] M. Borland, "Elegant: A Flexible SDDS-Compliant Code for Accelerator Simulation", *Advanced Photon Source LS-287*, September 2000.

[4] J. D. Bjorken and S. K. Mtingwa, "Intrabeam Scattering", *Part. Acc.*, vol. 13, pp. 115-143, 1983.